

Predicting $F_2^{D(3)}$ from the colour glass condensate model

J. R. Forshaw^a, R. Sandapen^b and G. Shaw^a

^aTheoretical Physics Group, Department of Physics and Astronomy,
The University of Manchester, M13 9PL, UK

^bTheoretical Physics Group, Department of Physics, Engineering Physics and Optics
Laval University, G1K 7P4, Quebec, Canada.

We confront the colour glass condensate motivated dipole model parameterization of Iancu, Itakura and Munier with the available HERA data on the diffractive structure function $F_2^{D(3)}$ and with existing dipole model parameterizations. Reasonably good agreement is found with only two adjustable parameters. We caution against interpreting the success of the model as compelling evidence for low- x perturbative saturation dynamics.

1. Introduction

Some years ago, it was shown [1, 2] that two phenomenological colour dipole models - the saturation model of Golec-Biernat and Wüsthoff [3] and the two-component model of Forshaw, Kerley and Shaw [4] - yielded a rather good description of the diffractive deep inelastic scattering (DDIS) data [5, 6]. These successes were achieved without adjusting any of the parameters of the models, which had been previously determined by fits to the deep inelastic structure function data at small- x [3, 4]. In both cases the DDIS structure function $F_2^{D(3)}(\beta, x, Q^2)$ was found to be dominated by the $q\bar{q}$ dipole contribution at large β , corresponding to diffractively produced states with invariant mass $M_X^2 \ll Q^2$, but at small β , corresponding to $M_X^2 \gg Q^2$, a $q\bar{q}g$ contribution becomes important (see below). Subsequently, both models have been successfully applied to a variety of other processes [7, 8, 9, 10, 11].

More recently a new colour dipole model, the colour glass condensate (CGC) model of Iancu, Itakura and Munier [12], has aroused considerable interest. This model can be thought of as a development of the Golec-Biernat–Wüsthoff saturation model. However, while still largely a phenomenological parameterisation, the authors claim that it contains the main features of the “color glass condensate” regime, where the gluon densities are high and non-linear effects become important. The parameters of the model have again been fixed by fitting the structure function data, which are now extremely precise, and the model has subsequently been shown to yield a good description of both ρ , ϕ [9] and J/Ψ [10] electroproduction data, with reasonable choices for the vector meson wavefunctions. However it has not yet been applied to DDIS, an omission which we propose to rectify in this short paper.

2. The CGC model for $F_2(x, Q^2)$

In the colour dipole model (Fig. 1), the dipole cross-section $\sigma_d(s^*, r, \alpha)$ is related to the photon-proton cross-section via

$$\sigma_{\gamma^* p}^{L,T} = \int d\alpha d^2r |\psi_{L,T}(\alpha, r)|^2 \sigma_d(s^*, r, \alpha) \quad (1)$$

where r is the transverse separation of the $q\bar{q}$ pair, α is the fraction of the incoming photon light-cone energy carried by the quark, and the variable s^* is chosen to be either $s = W^2$, the squared CMS energy of the photon-proton system, or the Bjorken scaling variable x . Henceforth we assume that the dipole cross-section is independent of α , i.e. we write $\sigma_d(s^*, r)$.

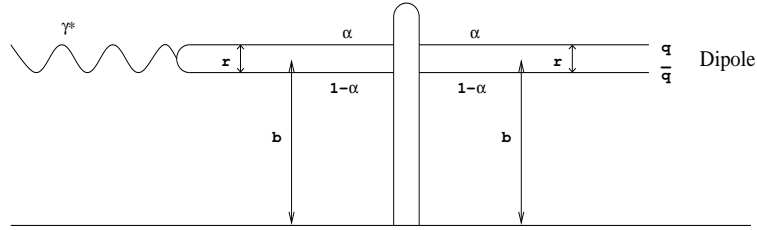


Figure 1. The dipole model for $F_2(x, Q^2)$.

In the CGC model, $s^* = x$ and the longitudinal and transverse components of the light-cone photon wave function are assumed to be given by the tree level QED expressions [13, 14]:

$$|\psi_L(\alpha, r)|^2 = \frac{6}{\pi^2} \alpha_{em} \sum_f e_f^2 Q^2 \alpha^2 (1 - \alpha)^2 K_0^2(\epsilon r) \quad (2)$$

$$|\psi_T(\alpha, r)|^2 = \frac{3}{2\pi^2} \alpha_{em} \sum_f e_f^2 \{ [\alpha^2 + (1 - \alpha)^2] \epsilon^2 K_1^2(\epsilon r) + m_f^2 K_0^2(\epsilon r) \} \quad (3)$$

where $\epsilon^2 = \alpha(1 - \alpha)Q^2 + m_f^2$, K_0 and K_1 are modified Bessel functions and the sum is over quark flavours f with quark masses m_f . The CGC dipole cross-section is assumed to be of the form

$$\begin{aligned} \sigma_d(x, r) &= 2\pi R^2 \mathcal{N}_0 \left(\frac{rQ_s}{2} \right)^{2[\gamma_s + \frac{\ln(2/rQ_s)}{\kappa\lambda\ln(1/x)}]} && \text{for} && rQ_s \leq 2 \\ &= 2\pi R^2 \{1 - \exp[-a \ln^2(brQ_s)]\} && \text{for} && rQ_s > 2, \end{aligned} \quad (4)$$

where the saturation scale $Q_s \equiv (x_0/x)^{\lambda/2}$ GeV. The coefficients a and b are uniquely determined by ensuring continuity of the cross-section and its first derivative at $rQ_s = 2$. The leading order BFKL equation fixes $\gamma_s = 0.63$ and $\kappa = 9.9$. The coefficient \mathcal{N}_0 is strongly correlated to the definition of the saturation scale and the authors find that the

quality of fit to F_2 data is only weakly dependent upon its value. For a fixed value of \mathcal{N}_0 , there are therefore three parameters which need to be fixed by a fit to the structure function data, i.e. x_0 , λ and R . In this paper, we take $N_0 = 0.7$ and a light quark mass of $m_q = 140$ MeV, for which the fit values are $x_0 = 2.67 \times 10^{-5}$, $\lambda = 0.253$ and $R = 0.641$ fm. We take $x = Q^2/(Q^2 + W^2) \times (1 + 4m_q^2/Q^2)^*$ and for the charm quark contribution we take $m_c = 1.4$ GeV.

3. The CGC model for $F_2^{D(3)}$

To calculate the contribution of the quark-antiquark dipole to $F_2^{D(3)}$ we made use of expressions derived from a momentum space treatment. We calculate the contribution of the higher $q\bar{q}g$ Fock state using an effective two-gluon dipole description [1, 15]. Typical Feynman diagrams are shown in Figure 2.

Defining

$$\Phi_{0,1} \equiv \left(\int_0^\infty r dr K_{0,1}(\epsilon r) \sigma_d(x_{IP}, r) J_{0,1}(kr) \right)^2, \quad (5)$$

we have for the longitudinal and transverse $q\bar{q}$ components

$$x_{IP} F_{q\bar{q},L}^D(Q^2, \beta, x_{IP}) = \frac{3Q^6}{32\pi^4 \beta b} \cdot \sum_f e_f^2 \cdot 2 \int_{\alpha_0}^{1/2} d\alpha \alpha^3 (1-\alpha)^3 \Phi_0, \quad (6)$$

$$x_{IP} F_{q\bar{q},T}^D(Q^2, \beta, x_{IP}) = \frac{3Q^4}{128\pi^4 \beta b} \cdot \sum_f e_f^2 \cdot 2 \int_{\alpha_0}^{1/2} d\alpha \alpha (1-\alpha) \left\{ \epsilon^2 [\alpha^2 + (1-\alpha)^2] \Phi_1 + m_f^2 \Phi_0 \right\} \quad (7)$$

where the lower limit of the integral over α is given by $\alpha_0 = (1/2) \left(1 - \sqrt{1 - 4m_f^2/M_X^2} \right)$ and b is the slope parameter which, unless otherwise stated, we take to be 7.2 GeV^{-2} [16].

For the $q\bar{q}g$ term we have[†]

$$x_{IP} F_{q\bar{q}g}^D(Q^2, \beta, x_{IP}) = \frac{81\beta\alpha_S}{512\pi^5 b} \sum_f e_f^2 \int_\beta^1 \frac{dz}{(1-z)^3} \left[\left(1 - \frac{\beta}{z} \right)^2 + \left(\frac{\beta}{z} \right)^2 \right] \quad (8)$$

$$\times \int_0^{(1-z)Q^2} dk_t^2 \ln \left(\frac{(1-z)Q^2}{k_t^2} \right) \left[\int_0^\infty u du \sigma_d(u/k_t, x_{IP}) K_2 \left(\sqrt{\frac{z}{1-z} u^2} \right) J_2(u) \right]^2. \quad (9)$$

The normalization of this component is rather uncertain; unless otherwise stated we take $\alpha_S = 0.2$.

Plots of the contributions to $x_{IP} F_2^{D(3)}$ calculated from these expressions are compared with H1 1994 data [5] in Figure 3 and with the ZEUS 1994 data [6] in Figure 4. The CGC model predictions are shown as the solid black curves in each plot. Also shown for comparison are the predictions of the Golec-Biernat & Wüsthoff (GW) saturation model [1] and the predictions of the FKS model [4]. For the GW model, the curves are exactly as in [1] except that we use a diffractive slope $b = 7.2 \text{ GeV}^{-2}$ rather than the GW choice

*For the Q^2 values we consider in this paper, the mass correction is unimportant.

[†]Following [2], we have inserted a missing factor of $1/2$ compared with the expression in [1].

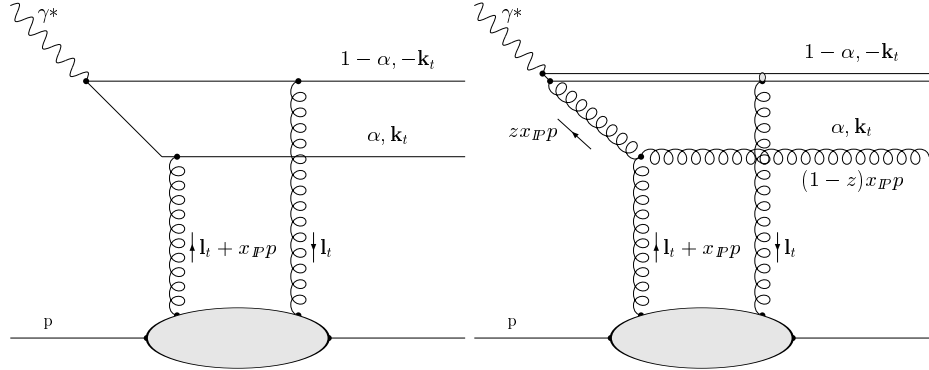


Figure 2. The $q\bar{q}$ and $q\bar{q}g$ contributions to $F_2^{D(3)}$.

of $b = 6 \text{ GeV}^{-2}$. For the FKS model we show two curves: the dashed red line uses the more compact parameterization of the dipole cross-section presented first in [7] whilst the blue dotted line is generated using the original ‘‘Fit 1’’ parameterization of [4]. As anticipated there is not much difference between the two FKS curves. There is also not very much difference between the CGC and GW curves, reflecting the fact that these two models use quite similar dipole cross-sections.

All our predictions contain no adjustable parameters in the dipole cross-section itself. However, we are free to adjust the forward slope for inclusive diffraction, b , within the range acceptable to experiment. This simply affects the overall normalization of $F_2^{D(3)}$. One can substantially improve the quality of the CGC fit to the data by lowering b towards the lower end acceptable to experiment, i.e. $b = 5.5 \text{ GeV}^{-2}$. We are also somewhat free to vary the value of α_s used to define the normalization of the $q\bar{q}g$ component, which enters at low to intermediate values of β , indeed choosing $\alpha_s = 0.15$ for the FKS model leads to a much improved fit. In Figure 5 we compare the CGC model, with the lower b parameter, and the FKS model, with the lower value of α_s , to the H1 data. Both models now agree rather well with the data.

Finally, in Figure 6 we show a breakdown of the CGC model, with the lower value of $b = 5.5 \text{ GeV}^{-2}$, into its various components and its comparison with the ZEUS data. The solid black line is again the total contribution whilst the blue dashed line is the contribution from $q\bar{q}$ dipoles (light quarks only), the red dotted line is the contribution from $c\bar{c}$ dipoles and orange dash-dot line is the contribution from the light quark dipoles produced by longitudinally polarized photons. We note that, in the region where the $q\bar{q}$ contribution is dominant (i.e. at larger values of β), approaches based upon the dipole model have very little room for manoeuvre. In particular, only the normalization is uncertain within the range allowed by the error on the measurement of the b parameter.

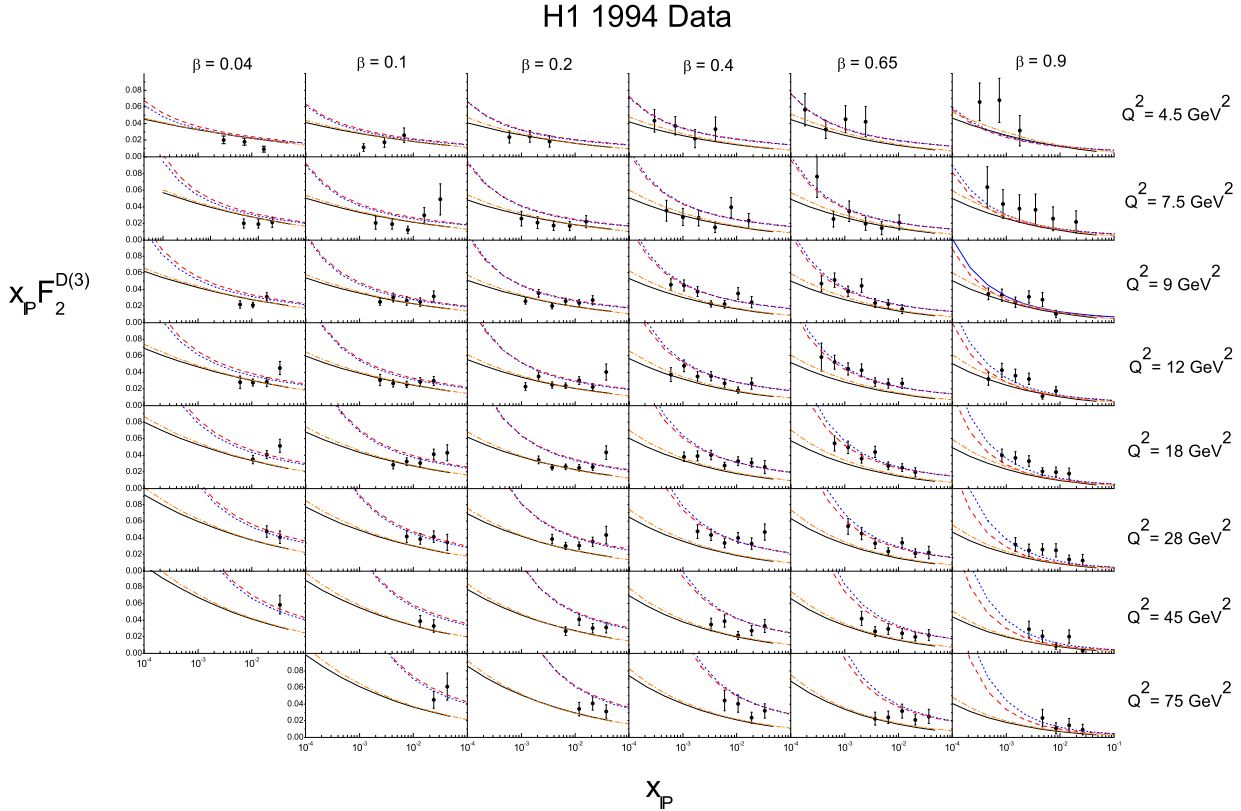


Figure 3. Predictions for $x_P F_2^{D(3)}$ compared with H1 1994 data. Solid black line: CGC model; Dashed red line: FKS (2002); Dotted blue line: FKS (1999); Dash-dot orange line: GW model.

4. Conclusions

We have used the dipole parameterization of Iancu, Itakura and Munier [12] to predict the diffractive structure function $F_2^{D(3)}$. This parameterization is anticipated to capture some of the essential dynamics of the colour glass condensate approach, in which saturation in x at fixed Q^2 is an essential feature. Agreement with the data is reasonably good provided that one accepts a forward slope for diffraction of 5.5 GeV^{-2} . We note that the CGC predictions are very similar to the previous predictions of Golec-Biernat & Wüsthoff [1]. In a previous paper, we have shown that the CGC model is also capable of describing the data on exclusive vector meson production [9].

However, we stress that the same data are also consistent with a “two pomeron” model [2, 4, 17] in which there is no low x saturation. Indeed Figure 5 of this paper compares the predictions of the FKS and CGC models to the $F_2^{D(3)}$ data. As such we conclude that

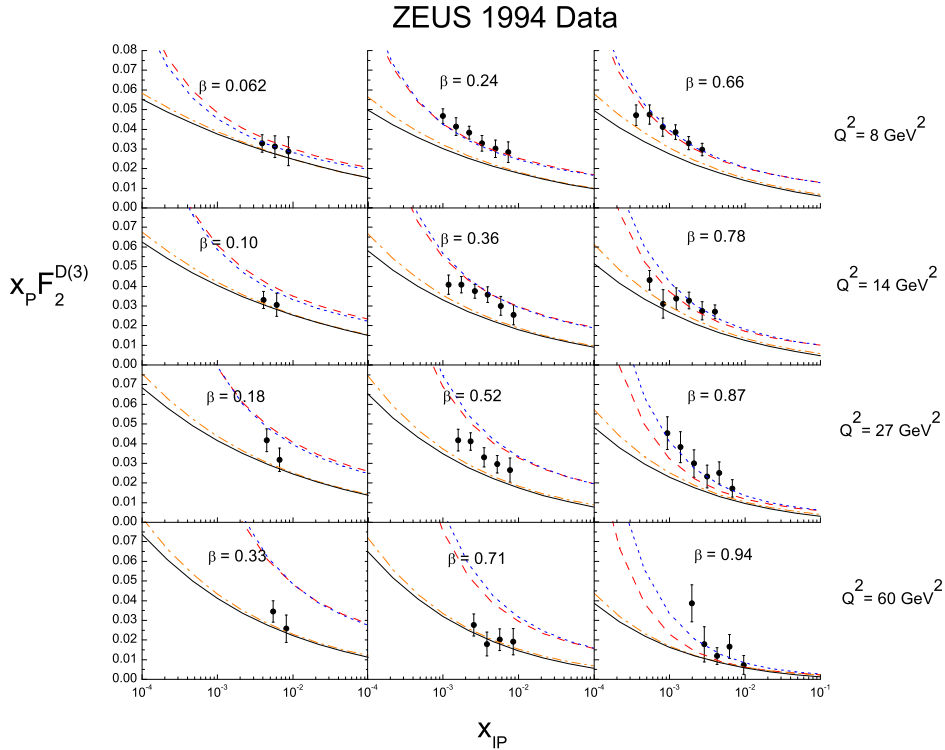


Figure 4. Predictions for $x_{IP}F_2^{D(3)}$ compared with ZEUS 1994 data. Solid black line: CGC model; Dashed red line: FKS (2002); Dotted blue line: FKS (1999); Dash-dot orange line: GW model.

the data are not yet precise enough, nor do they extend to sufficiently small values of x_{IP} , to discriminate between these very different theoretical approaches.

5. Acknowledgement

This research was supported in part by a UK Particle Physics and Astronomy Research Council grant number PPA/G/0/2002/00471.

REFERENCES

1. K. Golec-Biernat and M. Wüsthoff, Phys. Rev. **D60** (1999) 114023.
2. J.R. Forshaw, G. Kerley and G. Shaw, Nucl. Phys. **A675** (2000) 80.
3. K. Golec-Biernat and M. Wüsthoff, Phys. Rev. **D59** (1999) 014017.
4. J.R. Forshaw, G. Kerley and G. Shaw, Phys. Rev. **D60** (1999) 074012.
5. C. Adloff et al., H1 Collab., Zeit. Phys. **C76** (1997) 613.
6. J. Breitweg et al., ZEUS Collab., Eur. Phys. J. **C6** (1999) 43.

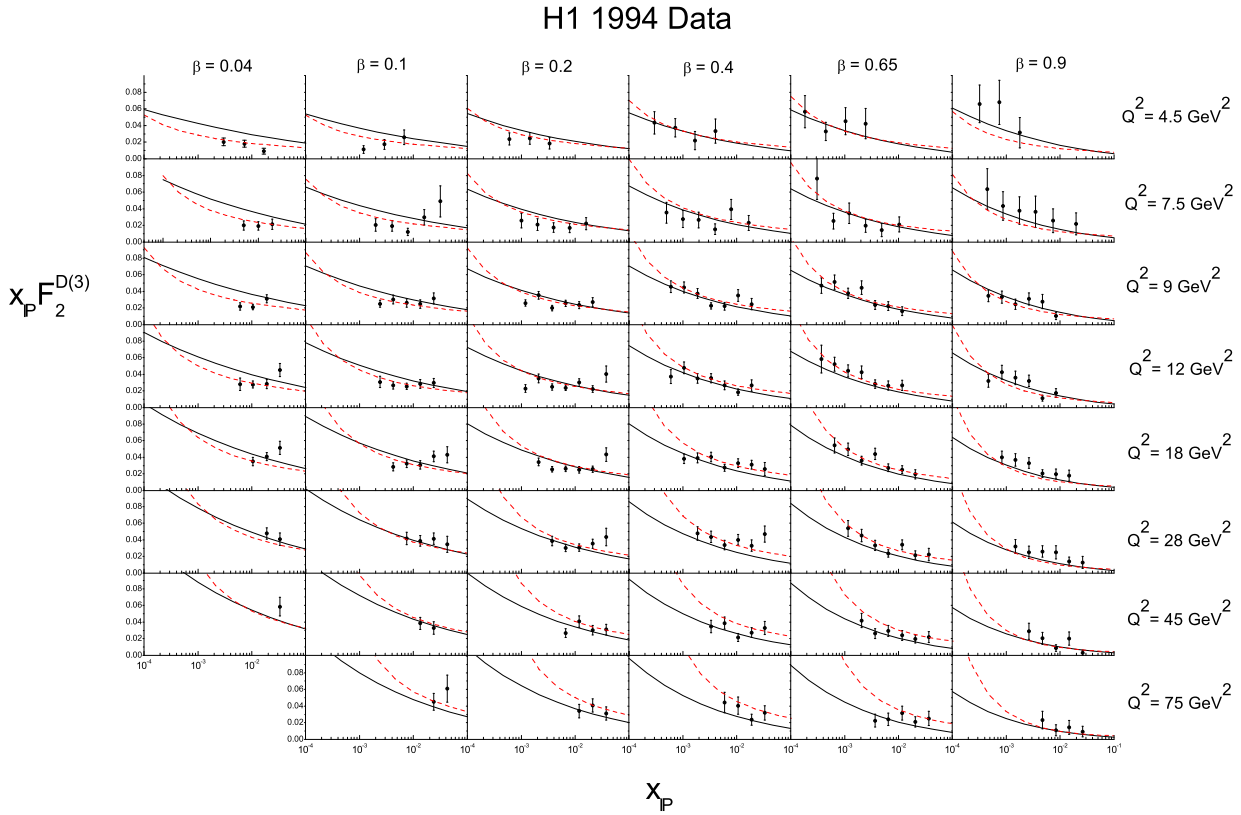


Figure 5. Predictions for $x_P F_2^{D(3)}$ compared with H1 1994 data after tuning the b parameter and α_s (see text). Solid black line: CGC model; Dashed red line: FKS (2002).

7. M.F. McDermott, R. Sandapen and G. Shaw, Eur. Phys. J. **C22** (2002) 665.
8. L. Favart and M. V. Machado, Eur. Phys. J. **C29** (2003) 365.
9. J.R. Forshaw, R. Sandapen and G. Shaw, Phys. Rev. D (to be published), hep-ph/0312172.
10. J.R. Forshaw, R. Sandapen and G. Shaw, in preparation.
11. A. C. Caldwell and M. S. Soares, Nucl. Phys. **A696** (2001) 125.
12. E. Iancu, K. Itakura and S. Munier, hep-ph/0310338.
13. N.N. Nikolaev and B.G. Zakharov, Z. Phys. **C49** (1991) 607.
14. H.G. Dosch, T. Gousset, G. Kulzinger and H.J. Pirner, Phys. Rev. **D55** (1997) 2602.
15. M. Wüsthoff, Phys. Rev. **D56** (1997) 4311.
16. J. Breitweg et al, ZEUS Collab., Eur. Phys. J. **C1** (1998) 81.
17. A. Donnachie and P.V. Landshoff, Phys. Lett. **B437** (1998) 408; ibid. **B470** (1999) 243; ibid. **B478** (2000) 146; ibid. **B518** (2001) 63.

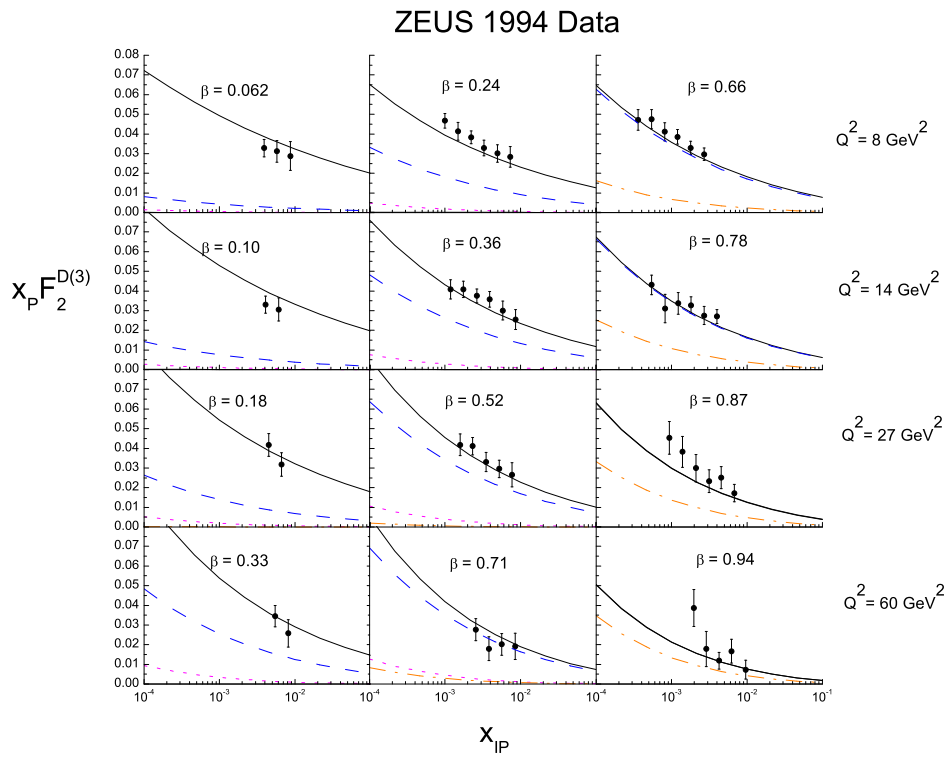


Figure 6. Various contributions to $x_{IP} F_2^{D(3)}$ compared with ZEUS 1994 data using the CGC dipole model. Solid black line: Total contribution; Dashed blue line: $q\bar{q}$ contribution; Dotted red line: $c\bar{c}$ contribution; Dashed-dotted orange line: longitudinal $q\bar{q}$ contribution.